DOI: 10.1002/ejic.200700652

# Amphiphilic Iron(II) and Nickel(II) Complexes Based on Alkylated Diazaoxa- and Triazacyclononane

David Domínguez-Gutiérrez,[a] Erika Eiser,[a] and Cornelis J. Elsevier*[a]

**Keywords:** Iron complexes / Nickel complexes / Macrocyclic ligands / Self-assembly / Metalloaggregates

It is known that including a metal into a micellar solution enhances both the colour and catalytic potential of such systems. This fact is well exemplified by the broad use of surfactant species as phase-transfer catalysts. In the present work, we report our studies concerning the aggregation properties of a series of iron and nickel-based triazacyclononane metalloamphiphiles. Upon multiple alkylation of the triazamacrocycle, we were able to obtain amphiphilic complexes that aggregate in toluene. We characterised the sizes and shapes of the aggregates by dynamic light scattering while their nature was assessed by atomic force microscopy.

## Introduction

Since the last half of the pervious century, there has been tremendous interest in the field of metal complexes based on macrocyclic ligands and investigations have undergone an important increase due to the relevance of many of these molecular systems.[1,2] The scope for this is rooted in well established chemistry and yet continuously offers new findings. Steric and electronic factors can be subtly varied in order to provide target complexes with high thermodynamic stabilities as well as magnetic and redox properties. In addition, the advantage of their synthetic flexibility is mostly used to prepare low-molecular weight compounds of bioinorganic importance.[3–5]

Large macrocycles (15-membered rings) show limited affinity for metal ions, $Ni^{II}$, $Cu^{II}$ and $Zn^{II}$ in particular, and this affinity is even lower than for open chain ligands with comparable structures. The reason is the large diameters of the cavities which exceed those of the small ions. Therefore, we decided not to study large macrocycles but turned instead to the use of smaller nine-membered rings which would yield more stable complexes with the envisaged metal ions. The $Fe(R_3TACN)$ moiety is very robust and tolerates the introduction of various reactive co-ligands in contrast to monodentate $(R_3N)_3$-Fe derivatives.

TACN-based (Figure 1) compounds have proven particularly useful in the characterisation of metals involved in dioxygen activation, as exemplified by the studies of Wieghardt[6] and Tolman.[7,8] In terms of catalytic activity, TACN has been demonstrated to be a more selective catalyst in styrene and methylacrylate polymerisation reactions[9] than larger macrocycles.[10]

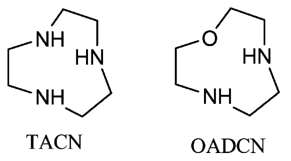

Figure 1. TACN = 1,4,7-triazacyclononane; ODACN = 1-oxa-4,7-diazacyclononane.

In the past, N-based macrocycles have been successfully used in the synthesis of both surfactants[11] and metalloamphiphiles.[12] Fallis and co-workers reported stable metalloamphiphiles based on tri- and tetraazacyclononyl ligands that self-aggregate in aqueous solutions.[12,13] We are interested in the synthesis of metalloamphiphiles that self-assemble into *inverted* aggregates because of their applications in catalysis. In inverted systems, the metalloamphiphiles can be brought into contact with larger amounts of organic substrates in comparison with water-based systems.[14] In order to obtain metalloamphiphiles that form inverted aggregates, ligand design and the choice of the solvent are very important.[15]

## Results and Discussion

The synthesis of the parent ligand 1,4,7-triazacyclononane, TACN, was first reported in very low yields by Yoshino et al.[16] For the synthesis of TACN and its alkylation (Scheme 1, 27% yield), we used a combination of procedures reported by other groups.[17–19] Mono- and trialkylation of TACN derivatives can be selectively performed although it is easier, however, to obtain trisubstituted derivatives than monosubstituted ones similar to the ligands syn-

---

[a] Van 't Hoff Institute for Molecular Chemistry, Universitet van Amsterdam,
Nieuwe Achtergracht 166, 1018 WV, Amsterdam, The Netherlands
E-mail: elsevier@science.uva.nl

thesised by White and co-workers.[20] In our case, the synthesis proceeds under reflux in diisopropylethyl amine as the solvent (as well as assisting base) over 3 d. The overall yield for the synthesis of $R_3$-TACN (**1**) was 17% (Scheme 1).

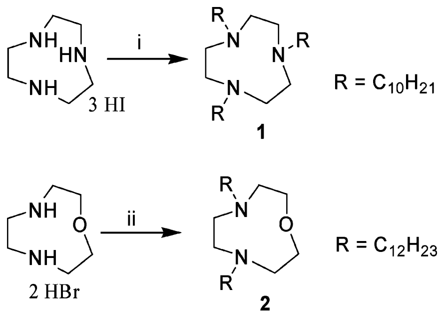

Scheme 1. Ligands $R_3$-TACN (**1**) and $R_2$-ODACN (**2**): (i) $C_{10}H_{21}Br$, *i*$Pr_2NEt$, 125 °C; (ii) $C_{12}H_{25}Br$, *i*$Pr_2NEt$, $CH_3CN$, reflux.

The synthesis of ODACN (the oxa-diaza counterpart of TACN) proceeds more easily than that of TACN. The procedure reported by Bowman and co-workers is, for the time being, the most efficient resulting in high yields for this ligand (*ca.* 80%).[21] All steps proceed with good yields, including the alkylation, resulting in compound **2** with an overall yield of 24% (Scheme 1).

The particular symmetry of the TACN ligand, when it acts as a tridentate ligand, always results in complexes where two of the *N*-alkyl hydrocarbon chains are in a relative *anti* disposition with regards to the third, thereby affecting the aggregation behaviour of the resultant molecules. Hence, for symmetry reasons, we also decided to synthesise complexes using the ODACN ligand as a building block. Clearly these complexes will lack one chain with respect to those containing TACN-type ligands but we assumed that this would be the most appropriate alternative to build tridentate macrocyclic ligands with two tails. In addition, to the best of our knowledge, no ODACN-type ligands have been reported to form polynuclear complexes, which could favour the formation of smaller aggregates.[22–25] In this way, an additional advantage is that the resultant molecular structures as well as the aggregates constituted from them are expected to be less complex.

Encouraged by the positive results obtained by Fallis et al.[12] in the synthesis of metallosurfactants that self-assemble in aqueous solutions, we employed ligand **1** in the syntheses of iron and nickel complexes aiming at the formation of inverted aggregates, preferably inverted micelles. The synthesis of **3** is depicted in Scheme 2: $FeCl_2$ was treated with ligand **1** in ethanol at ambient temperature over several days to give **3** in 57% yield.

We analysed complex **3** by $^{13}C$ NMR spectroscopy and mass spectrometry, while its purity was confirmed by elemental analysis. The structure of **3** proposed here is based on the mass spectrometric analysis and by analogy with that described by other groups.[26–28] The cation $[Fe_2(\mu\text{-}Cl)_3(L)_2]^+$ (L = $R_3$-TACN) has been previously characterised by Wieghardt et al.[26] and its structure corresponds to a face-sharing bioctahedral geometry. As reported, the facility and efficiency of this conversion suggests that the $Cl^-$ ligands in $[Fe(L)Cl_3]^-$ are kinetically labile and tend to promote the formation of bridged species.

The synthesis of **4** (Scheme 3) was carried out in a way analogous to that of **3** in 48% yield, using $Fe(NO_3)_3$ as the metal source and ethanol as a solvent. It exhibited broad lines in its $^1H$ NMR spectrum. The structure of **4** was established by $^{13}C$ NMR spectroscopy, mass spectrometry and elemental analysis. Its structure has been proposed on the basis of the combined analyses, particularly its field desorption mass spectrum in which the main peak has been assigned to the ion $[Fe_2(\mu\text{-}O)(H_2O)_4(R_3TACN)_2](NO_3)_3]^+$.

$$3\ FeCl_2 + 3\ R_3\text{-TACN} \rightarrow [(R_3\text{-}\ TACN)_2Fe_2(Cl)_3{}^+][(R_3\text{-}\ TACN)FeCl_3{}^-]$$

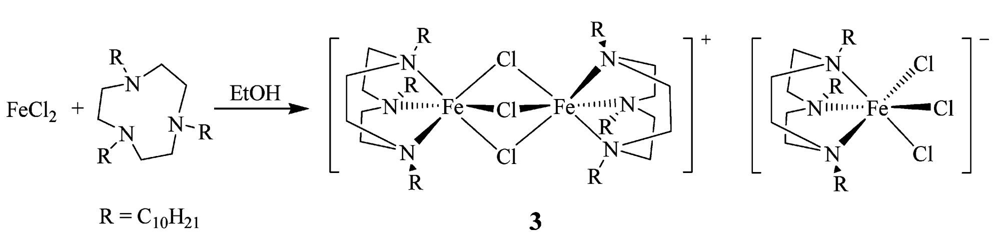

**3**

Scheme 2. Synthesis of an $Fe^{II}$ complex with **1**, an $R_3$-TACN ligand.

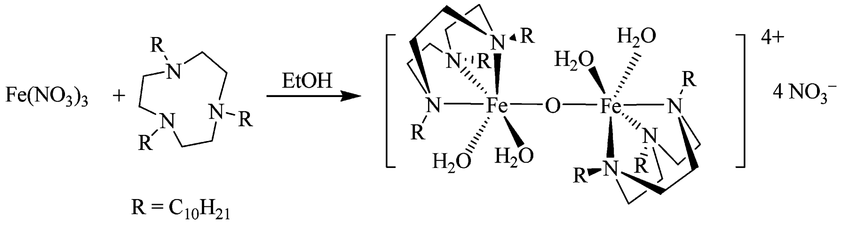

**4**

Scheme 3. Synthesis of complex **4**.

In a similar manner, complex **5** resulted from reaction of ligand **1** with $NiCl_2$ (see Scheme 4) in ethanol. Analogous to **4**, the structure of this complex was proposed on the basis of the mass spectrum (field desorption) of its solution in $CH_2Cl_2$ which showed only a strong signal attributable to $[Ni_2(\mu\text{-}Cl)_3(L)_2]^+$. In principle, an alternative structure is $[Ni_2Cl_2(\mu\text{-}Cl)_2(L)_2]$ and this would be composed from a pair of edge-sharing octahedra. However, previous studies[29] have indicated that for dinuclear metal halide adducts of 1,4,7-trimethyl-1,4,7-triazacyclononane, structures containing edge-sharing octahedra exhibit unfavourable steric interactions so that structures containing face-sharing octahedra (as in $[Ni_2(\mu\text{-}Cl)_3(Lx)_2]Cl$) are formed in preference.

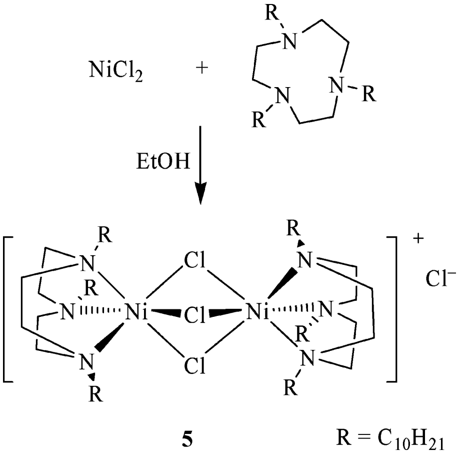

Scheme 4. Synthesis of an amphiphilic $Ni^{II}$ complex with ligand **1**.

Regardless of the metal used, TACN ligands bestow a defined shape on the resultant complexes since these ligands always coordinate in a facial manner. In this way, the metal is embedded in the ligand cavity and the tails point outwards. However, due to the configuration of the nine-membered ring, two of these chains will always be in the same plane whereas the third will be pointing into the opposite direction. With this situation, it will be impossible for the molecules to adopt the appropriate shape of a truncated cone[30] which may jeopardise the desired behaviour of these complexes, i.e. to pack into micellar pockets.

The syntheses of the metal complexes **6** and **7** carrying the ODACN unit proceed smoothly from the reaction of the ligand with the corresponding metal salt in ethanol at ambient temperature. The yields are 66% and 74%, respectively (Scheme 5). The complexes were characterised by $^{13}C$ NMR spectroscopy and mass spectrometry and their purity assessed by elemental analysis. The structures of both metal complexes were proposed based on their mass spectra (field desorption) obtained on $CH_2Cl_2$ solutions. These had signals attributable to $[M(L)(Cl)]^+$ as the main molecular peaks. There are no reports of bridged species with metal complexes bearing ODACN ligands in the literature.

We used DLS in order to obtain information about the sizes, shapes and polydispersities of the aggregates. In principle, it is desirable to employ a solvent of low polarity since it will trigger the self-assembly of amphiphilic compounds into inverted aggregates in cases where they possess both a strong shift in polarity and an appropriate geometry.

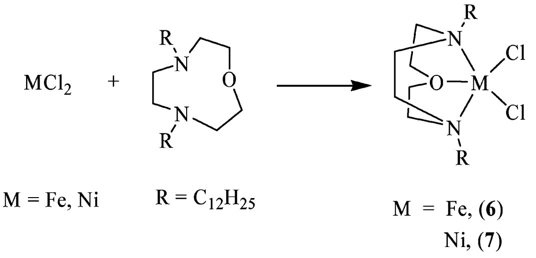

Scheme 5. Synthesis of $Fe^{II}$ and $Ni^{II}$ complexes with **2**.

Unfortunately, metal complexes **3**–**5** are not soluble in hexane or related solvents (cyclohexane, isooctane) so only toluene could be employed as a reference solvent. In this way, $10^{-3}$ M solutions in toluene of TACN-based complexes **3** to **5** were examined with DLS. In Figure 2, the distribution functions of both solutions are depicted. Only one type of aggregate is formed for **3** and **4**, their polydispersities being similar.

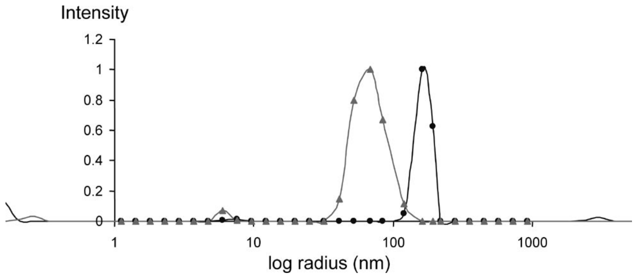

Figure 2. Size distributions in toluene of **3** (▲) and **4** (●).

The iron complexes self-aggregate but the nickel complex does not. The mean hydrophobic radii ($R_h$) measured by DLS are listed in Table 1. The aggregates formed in this way have large radii and they cannot therefore be micelles but must be larger structures. Examination of the samples using the cross-polariser on the dynamic light scattering device indicated that the structures are spherical. Knowing this, we can state that the structures are spherical inverted vesicles; they cannot form direct structures because the solvent is apolar.[15] Unexpectedly, even though the structures, the ligands and the ionic radii are the same, the nickel complexes do not aggregate while the iron complexes do. Unlike aqueous aggregates, TACN complexes aggregate when they contain late transition metals ($Ni^{II}$,[12] $Cu^{I}$[13]) but inverted aggregates certainly need different requirements and the metal centre is one of them. Several explanations can be given for this behaviour. When iron is complexed to TACN, the shift in polarity induced in the molecule is strong enough to trigger aggregation in apolar solvents. When considering compounds **3** and **5** in particular, changing the metal from iron to nickel would in principle make no appreciable difference in the aggregation behaviour, since they have the same ligands, the same coordination numbers, the same charges and similar ionic radii. Since their geometries are the same, the aggregation of **3** may be explained by its counterion which is the main difference with respect to compound **5**. In turn, compound **4** possesses a different structure that lies in the bridging oxygen, allowing the molecule to buckle, thereby finding a more adequate geometry for self-aggregation.

Table 1. DLS data for aggregates of complexes **3**–**5** in toluene[a].

| Complex | $R_h$ aggregates |
|---|---|
| $[Fe_2(\mu\text{-}Cl)_3(R_3TACN)_2]^+$ (**3**) | 69 ± 15 |
| $[Fe_2(\mu\text{-}O)(H_2O)_4(R_3TACN)_2]^{4+}$ (**4**) | 162 ± 20 |
| $[Ni_2(\mu\text{-}Cl)_3(R_3TACN)_2]^+$ (**5**) | none |

[a] Mean hydrophobic radii ($R_h$) in nm of $10^{-3}$ M solutions in toluene.

The aggregation behaviour of complexes **6** and **7** was studied in the same way as described for the TACN complexes. Similarly, they are not soluble in hexane or similar solvents. Hence, other apolar solvents such as toluene, diethyl ether and more polar ones such as $CHCl_3$ were employed but no aggregate formation was seen. No improvement was observed upon standing for 72 h or when using water as a (co-)solvent. There are several reasons for the lack of self-aggregation activity. One is due to the presence of only two instead of three alkyl chains that the TACN-based complexes have, so an appropriate hydrophilic/lyophilic balance is not achieved. However, if the chains do limit the aggregation to the apolar solvents, aggregates should have been obtained in aqueous solutions. Therefore, it is more likely that the lack of surface activity is due to the second reason, i.e, the nature of the ligand, particularly the ODACN moiety. Given the structures of **6** and **7** it is remarkable that they do not aggregate when compared with compounds of a similar shape to those studied by Fallis et al.[12]

It is not possible to derive the exact morphology of the aggregates from the exclusive use of DLS. Vesicles are structures constituted by at least one bilayer that closes onto itself (unilamellar vesicle) which at the same time could contain more bilayers inside (multilamellar vesicle). Another feasible option is the coalescence of several micelles and/or vesicles to render aggregates with larger sizes and more complex structures. AFM was used in order to establish whether any of these phenomena take place and also to gain understanding of the aggregates' morphologies. In this way, freshly prepared toluene solutions of **3**–**5** were deposited on mica, the toluene was allowed to evaporate and the aggregates were consequently left behind and examined.

AFM scans show that the deposited structures maintain a rather spherical shape in spite of the shear forces they undergo upon solvent evaporation (Figure 3). The radii offered by solid AFM slightly differ with respect to those in solution (DLS provides the hydrodynamic radius) because the aggregates are dry. The solvent that is in principle present in the surfactant interface and inside the aggregates has evaporated, causing the collapse of the structure, a phenomenon that can also contribute to the aggregates' disruption.

Larger aggregates than those formed by **4** maintain a more spherical shape than the smaller ones because they are more robust and thereby more resistant towards reshaping. AFM data obtained from the dry aggregates of **3** are depicted in Figure 3 showing that, as a general trend, the aggregates do not cover the surface homogeneously and are more polydispersed than those formed by **4**, as was expected from the DLS experiments (see Figure 2). There is nevertheless an important feature: the height of these aggregates is about 15 nm. A molecule of **3** with its fully extended chains has a length of ca. 4 nm meaning that an aggregate consists of approximately four stacks of molecules. In the first instance, this can be seen as an indication that the vesicles are bilamellar (formed by two bilayers). Alternatively, the data can also be interpreted as the less likely model of one big monolamellar vesicle that encapsulates another smaller monolamellar vesicle. Both interpretations are based on the same two layers with two stacks of complexes when the aggregates lay flat on the surface (see Figure 3). Additionally, AFM confirmed that the aggregates have the spherical shape predicted by DLS. The diameters found by AFM are smaller than obtained with DLS, while the values are close to those expected: ca. 45 nm for **3** and about 150 nm for **4** (see Table 1).

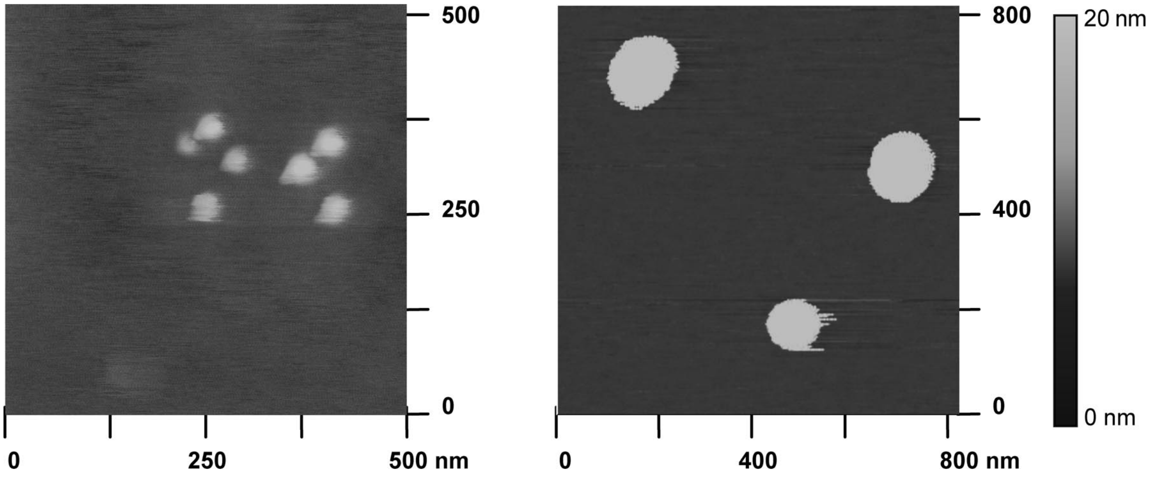

Figure 3. a) AFM height contrast picture of dry aggregates of **3** (left) and **4** (right).

Considering that compounds **3** and **4** are comprised of the same ligand, the nature of the so-formed aggregates should mainly be due to the counterions. In this way, the difference in size is due to the counterion effect: the more bulky $NO_3^-$ associated with **4** accounts for the formation of more expanded structures since they cannot pack into smaller aggregates. In fact, vesicles of **3** have half the size of those of **4** whereas, as seen with AFM, the height of the dry aggregates is the same. This means that both vesicles are bilamellar even though their sizes are different. Therefore, not only the nature of the ligand is crucial in determining the self-aggregation behaviour but also the counterions employed can dramatically alter the sizes of the resultant aggregates.

## Conclusion

We synthesised novel, amphiphilic complexes **3**–**5** containing a $R_3$-TACN ligand that may aggregate into inverted micelles. We have studied their self-aggregation properties with dynamic light scattering and atomic force microscopy. The iron complexes showed the formation of aggregates in toluene but no aggregation was observed when other solvents were employed. We postulate that the difficulty in undergoing self-assembly into smaller aggregates, such as inverted micelles, is caused by the unfavourable geometry of the complexes. Due to their dinuclear nature and the unfavourable arrangement of the tails, the complexes containing $R_3$-TACN ligands probably do not possess the desired truncated cone geometry necessary for an efficient micellar packing. Based on AFM images of dried samples on a solid support, the structure of the so-formed aggregates appeared to be inverted vesicles which consist of a double bilayer (bilamellar vesicles) that closes onto itself.

We then attempted to obtain inverted micelles by synthesising complexes containing the more symmetric $R_2$-ODACN ligand (**6**, **7**). Even though these complexes possess solubilities similar to complexes **3**–**5**, they did not aggregate in any solvent (polar or apolar). While all metal complexes presented herein are amphiphilic, self-aggregation was only observed in iron complexes containing the $R_3$-TACN ligand. A plausible reason for the observed differences can be attributed to differences in the geometries of the complexes, the role of the counterion, the nature of the polar head (TACN vs. ODACN) and, to a lesser extent, the transition metal employed.

By employing polyalkylated macrocyclic ligands, we have been able to obtain several metalloamphiphiles that are insoluble in water but are prone to aggregate into inverted vesicles in apolar solvents. In comparison to analogous metalloamphiphiles that self-aggregate in water, we have shown that it is possible to alter the aggregation behaviour of metalloamphiphiles by ligand design.

## Experimental Section

**Dynamic Light Scattering (DLS):** Measurements were carried out at 20 °C on a DLS set-up from ALV (Germany) with a wavelength ($\lambda_0$) of 632.8 nm. Angle-dependent measurements assured the purely diffusive nature of the aggregates formed. Solutions were measured immediately after filtration. The intensity data were normalised using toluene as a reference standard. Dispersions of compounds **3** to **7** (1 mM) were prepared by a brief sonication (10 min at room temp.) of the compounds in the corresponding bifiltered solvent. The resultant solutions were filtered using a 0.2 µm filter prior to measurements. Measurements at 70 °C were carried out using a Haake Phoenix II P2-C25P thermoregulatory bath.

**Atomic Force Microscopy (AFM):** AFM analysis of particles formed from the different solutions were carried out with a commercial atomic force microscope (NanoScope IIIa with MultiMode head, Veeco Instruments Inc., Münster, Germany). All the measurements were done in air using the "tapping mode" of the AFM. The images were taken with a silicon cantilever (BS-Tap300, Budgetsensors) with a resonant frequency of about 330 kHz and a spring constant of about 40 $Nm^{-1}$. Solutions were prepared analogously to those used for DLS measurements. A 10 µL aliquot of fresh solution was deposited onto a small piece (1 cm × 1 cm) of freshly cleaved mica and allowed to dry for a few minutes.

**General:** All synthetic experiments were performed under dry nitrogen using standard Schlenk techniques, unless otherwise stated. All non-deuterated solvents, reagent grade or better were dried according to standard previous procedures under nitrogen. Deuterated solvents were used as received. $^1H$ and $^{13}C\{^1H\}$ NMR spectra were recorded at 300.13 and 75.48 MHz, respectively, using a Varian Unity 300 MHz spectrometer. Unless otherwise stated, the NMR measurements were performed in $CDCl_3$. $^1H$ and $^{13}C\{^1H\}$ NMR spectra are reported in parts per million high frequency from an external reference of tetramethylsilane. Fast Atom Bombardment (FAB) mass spectrometry was carried out using a JEOL JMS SX/SX 102A four-sector mass spectrometer, coupled to a JEOL MS-MP9021D/UPD system program. Samples were loaded in a matrix solution (3-nitrobenzyl alcohol) on to a stainless steel probe and bombarded with xenon atoms with an energy of 3 keV. The high resolution FAB-MS measurements were executed with a resolving power of 10,000 (10% valley definition). Commercially available reagents were used as received. 1,4,7-triazacyclononane trihydroiodide salt[27] and 1,4-diaza-7-oxacyclononane bis(hydrobromide salt)[21] were synthesised following published procedures.

**1,4,7-Tridecyl-1,4,7-triazacyclononane, ($R_3$-TACN) (1):** 1,4,7-triazacyclononane trihydroiodide salt (5 g, 9.7 mmol) was suspended in diethyl ethylamine (20 mL) and stirred for 10 min. To this solution, *n*-decylbromide (8.7 g, 38.8 mmol) was added, stirred for 1 d at ambient temperature and then at 125 °C for 3 d. Volatiles were removed under vacuum, redissolved in $CH_2Cl_2$, (30 mL) and extracted with water (3× 20 mL). The organic extract was dried with $Na_2SO_4$, filtered, the solvent evaporated and the crude product chromatographed on silica gel with a $CH_2Cl_2/Et_3N$ (95:5) mixture rendering **1** as a yellowish oil. Yield 3.3 g (62%). $^1H$ NMR: $\delta$ = 0.79 (t, $^2J_{H,H}$ = 7.8 Hz, 9 H, $CH_3$), 1.17–1.40 [br. m, $CH_3(CH_2)_8$-$CH_2N$, 48 H], 2.36 (t, $^2J_{H,H}$ = 8.1 Hz, 6 H,$CH_2N$), 2.65 (s, 12 H, $NCH_2CH_2N$) ppm. $^{13}C\{^1H\}$ NMR: $\delta$ = 14.3 ($CH_3$), 22.8 ($CH_3CH_2$), 27.7 ($CH_2CH_2CH_2N$), 28.0 ($CH_2CH_2CH_2N$), 29.8 [br. s, $CH_3(CH_2)_2(CH)_5$], 32.1 ($CH_3CH_2CH_2$), 46.4 [$(CH)_8CH_2N$], 55.6 ($NCH_2CH_2N$) ppm.

**1,4-Didodecyl-7-oxa-1,4-diazacyclononane (2):** 7-Oxa-1,4-diazacyclononane bis(hydrobromide) salt (10.0 g, 34.24 mmol) was added to a solution of *N*,*N'*-bis(isopropyl)ethylamine (17.70 g, 136.98 mmol) in acetonitrile (200 mL) and the mixture stirred for 1 h at room temperature. 1-Dodecylbromide (21.77 g, 85.6 mmol) was added and the reaction heated to reflux for 16 h. The solvent was evaporated, the residue dissolved in diethyl ether (25 mL), washed with water (2× 10 mL) and purified with flash chromatography on silica gel with $CH_2Cl_2/Et_3N$ (95:5) to afford a colourless oil. Yield 10.0 g (62%). $^1H$ NMR: $\delta = 0.86$ (t, $^2J_{HH} = 7.5$ Hz, 6 H, $CH_3$), 1.7–1.1 [m, 40 H, $CH_3(CH_2)_8CH_2N$], 2.48 [t, $^2J_{H,H} = 7.5$ Hz, 4 H, $CH_3(CH_2)_8CH_2N$], 2.72 (s, 4 H, $NCH_2CH_2N$), 2.76 (t, $^2J_{H,H} = 4.2$ Hz, 4 H, $NCH_2CH_2O$), 3.69 (d, $^2J_{H,H} = 4.2$ Hz, 4 H, $OCH_2CH_2O$) ppm. $^{13}C\{^1H\}$ NMR: $\delta = 14.3$ ($CH_3$), 22.9 ($CH_3CH_2$), 27.7 ($CH_2CH_2CH_2N$), 28.1 ($CH_2CH_2CH_2N$), 29.8 br. s [$CH_3(CH_2)_2(CH)_5$], 32.1 ($CH_3CH_2CH_2$), 55.5 ($CH_2CH_2CH_2N$), 55.7 ($NCH_2CH_2N$), 58.7 ($NCH_2CH_2O$), 72.9 ($OCH_2CH_2O$) ppm.

**$[Fe_2(R_3\text{-TACN})_2(Cl)_3][Fe(R_3\text{-TACN})(Cl)_3]$ (3):** $FeCl_2(H_2O)_4$ (30 mg, 0.151 mmol) and **1** (83 mg, 0.151 mmol) were dissolved in dry ethanol (10 mL). The mixture was stirred for 16 h at 40 °C, turning yellowish in the process. The resultant solution was filtered and the solvent evaporated. The crude product was redissolved in diethyl ether and filtered twice through a 0.2 µm pore size LC13 PVDF filter. Volatiles were evaporated and the resultant light yellow product was dried in vacuo. Yield 54 mg (57%). $^{13}C\{^1H\}$ NMR ($CD_2Cl_2$): $\delta = 14.3$ ($CH_3$), 22.9 ($CH_3CH_2$), 27.7 ($CH_2CH_2CH_2N$), 27.9 ($CH_2CH_2CH_2N$), 29.6 br. s [$CH_3(CH_2)_2(CH)_5$], 32.2 ($CH_3CH_2CH_2$), 46.9 [$(CH)_8CH_2N$], 58.1 ($NCH_2CH_2N$) ppm. MS (FAB$^+$): $m/z$ = 1175.8123 [$Fe_2(\mu\text{-Cl})_3(R_3\text{-TACN})_2$]$^+$, 1140.3159 [$Fe_2(\mu\text{-Cl})_2(R_3\text{-TACN})_2$]H$^+$ 709.4296 [$Fe(Cl)_3(R_3\text{-TACN})$]H$^+$. $C_{98}H_{204}Cl_6N_9Fe_3$ (1885.24): calcd. C 62.31, H 10.89, N 6.67; found C 62.60, H 11.03, N 6.35.

**$[Fe_2(\mu\text{-O})(H_2O)_4(R_3\text{-TACN})_2](NO_3)_4$ (4):** Synthesis and purification are analogous to those of **3** but $Fe(NO_3)_3(H_2O)_9$ (40 mg, 0.10 mmol) and $R_3$-TACN (55 mg, 0.10 mmol) were used instead. Yield 73 mg (48%). $^{13}C\{^1H\}$ NMR ($CD_2Cl_2$): $\delta = 14.3$ ($CH_3$), 22.8 ($CH_3CH_2$), 27.8 ($CH_2CH_2CH_2N$), 28.0 ($CH_2CH_2CH_2N$), 29.7 [br. s, $CH_3(CH_2)_2(CH)_5$], 32.1 ($CH_3CH_2CH_2$), 46.6 [$(CH)_8CH_2N$], 58.5 ($NCH_2CH_2N$) ppm. MS (FAB$^+$): $m/z$ = 1487.0786 [MH]$(NO_3)_3^+$, 1425.0908 [MH]$(NO_3)_2^+$. $C_{72}H_{158}Fe_2N_{10}O_{17}$ (1547.05): calcd. C 55.87, H 10.29, N 9.05; found C 55.83, H 10.41, N, 8.86.

**$[Ni_2(\mu\text{-Cl})_3(R_3\text{-TACN})_2]Cl$ (5):** Synthesis and purification are analogous to those of **3** but $NiCl_2(H_2O)_6$ (36 mg, 0.151 mmol) and **1** (83 mg, 0.151 mmol) were employed and the solution turned light green. Yield 32 mg (63%). $^{13}C\{^1H\}$ NMR ($CD_2Cl_2$): $\delta = 14.5$ ($CH_3$), 23.0 ($CH_3CH_2$), 28.2 ($CH_2CH_2CH_2N$), 28.4 ($CH_2CH_2CH_2N$), 30.2 [br. s, $CH_3(CH_2)_2(CH)_5$], 32.7 ($CH_3CH_2CH_2$), 47.7 [$(CH)_8CH_2N$], 59.0 ($NCH_2CH_2N$) ppm. MS (FAB$^+$): $m/z$ = 1320.9769 [$Ni_2(\mu\text{-Cl})_3(R_3\text{-TACN})_2$]$^+$, 1287.0165 [$Ni_2(\mu\text{-Cl})_2(R_3\text{-TACN})_2$]H$^+$. $C_{72}H_{150}Cl_4N_6Ni_2$ (1354.94): calcd. C 63.62, H 11.12, N 6.18; found C 63.71, H 11.44, N 6.08.

**$[FeCl_2(R_2\text{-ODACN})]$ (6), $[NiCl_2(R_2\text{-ODACN})]$ (7):** Similarly to **3**, $FeCl_2(H_2O)_4$ or $NiCl_2(H_2O)_6$ (0.15 mmol) and $R_2$-ODACN (62 mg, 0.15 mmol) were dissolved in dry ethanol (10 mL) and stirred for 16 h at ambient temperature. The resultant solution was filtered and the solvent evaporated. The crude product was chromatographed on Sephadex LH20 using 2-propanol as eluent. The solvent was evaporated and the resultant product dried in vacuo.

**Analytical Data for 6:** Yield 53 mg (66%). $^{13}C\{^1H\}$ NMR ($CD_2Cl_2$): $\delta = 14.3$ ($CH_3$), 22.8 ($CH_3CH_2$), 27.4 ($CH_2CH_2CH_2N$), 28.3 ($CH_2CH_2CH_2N$), 29.8 [br. s, $CH_3(CH_2)_2(CH)_5$], 32.2 ($CH_3CH_2CH_2$), 57.0 ($CH_2CH_2CH_2N$), 57.9 ($NCH_2CH_2N$), 60.3 ($NCH_2CH_2O$), 76.5 ($OCH_2CH_2O$) ppm. MS (FAB$^+$): $m/z$ = 503.34 [MH – Cl]$^+$. $C_{26}H_{54}Cl_2FeN_2O$ (536.30): calcd. C 58.10, H 10.13, N 5.21; found C 58.05, H 10.16, N 5.09.

**Analytical Data for 7:** Yield 60 mg (74%). $^{13}C\{^1H\}$ NMR ($CD_2Cl_2$): $\delta = 14.3$ ($CH_3$), 22.8 ($CH_3CH_2$), 27.7 ($CH_2CH_2CH_2N$), 28.5 ($CH_2CH_2CH_2N$), 29.9 [br. s, $CH_3(CH_2)_2(CH)_5$], 32.0 ($CH_3CH_2CH_2$), 57.6 ($CH_2CH_2CH_2N$), 58.2 ($NCH_2CH_2N$), 61.1 ($NCH_2CH_2O$), 77.3 ($OCH_2CH_2O$) ppm. MS (FAB$^+$): $m/z$ = 505.34 [MH – Cl]$^+$. $C_{26}H_{54}Cl_2N_2NiO$ (538.30): calcd. C 57.80, H 10.07, N 5.18; found C 58.11, H 10.09, N 5.20.

## Acknowledgments

Daniel Ebeling from the Physikalisches Institut, Westfälische Wilhelms Universität Münster (Germany) is kindly acknowledged for performing the AFM measurements. D. D.-G. and C. J. E. thank National Research School, Combination Catalysis Controlled by Chemical Design (NRSC-Catalysis) for financial support, project number 2001-10. We are indebted to the reviewers for their constructive criticism and assistance.

[1] P. Deslongchamps, Y. Dory, G. Berthiaume, L. Ouellet, R. Lan, *PCT Int. Appl.* **2001**.
[2] G. A. Melson, *Coordination Chemistry of Macrocyclic Compounds*; Plenum: New York, **1979**.
[3] U. Bossek, H. Hummel, T. Weyhermueller, K. Wieghardt, S. Russell, L. van der Wolf, U. Kolb, *Angew. Chem. Int. Ed. Engl.* **1996**, *35*, 1552–1554.
[4] N. H. Williams, *J. Chem. Soc.* **2000**, *122*, 12023–12024.
[5] A. V. Xavier, *Frontiers in Bioinorganic Chemistry*; VCH, Weinheim, **1986**.
[6] R. Schneider, T. Justel, K. Wieghardt, B. Z. Nuber, *Z. Naturforsch., A: Phys. Sci.* **1994**, *49*, 330–336.
[7] J. A. Halfen, S. Mahapatra, E. C. Wilkinson, S. Kaderli, V. G. Young, L. Que, A. Zuberbuhler, W. B. Tolman, *Science* **1996**, *271*, 1397–1400.
[8] J. A. Halfen, W. B. Tolman, K. Weighardt, *Inorg. Synth.* **1998**, *32*, 75–81.
[9] J. Z. X. Xia, K. Matyjaszewski, in *Transition Metal Catalysis in Macromolecular Design*, Am. Chem. Soc., Washington, DC, **2000**, vol. 13, p. 207–223.
[10] M. Teodorescu, K. Matyjaszewski, *Macromolecules* **1999**, *32*, 4826–4831.
[11] A. D. Pidwell, S. R. Collinson, S. J. Coles, M. B. Hursthouse, M. Schroder, D. W. Bruce, *Chem. Commun.* **2000**, 955–956.
[12] I. A. Fallis, P. C. Griffiths, P. M. Griffiths, D. E. Hibbs, M. B. Hursthouse, A. L. Winnington, *Chem. Commun.* **1998**, 665–666.
[13] P. C. Griffiths, I. A. Fallis, D. J. Willock, A. Paul, C. L. Barrie, P. M. Griffiths, G. M. Williams, S. M. King, R. K. Heenan, R. Gorgl, *Chem. Eur. J.* **2004**, *10*, 2022–2028.
[14] M. Fanti, F. Mancin, P. Tecilla, U. Tonellato, *Langmuir* **2000**, *16*, 10115–10122.
[15] D. Dominguez-Gutierrez, M. Surtchev, E. Eiser, C. J. Elsevier, *Nano Lett.* **2006**, *6*, 145–147.
[16] H. Koyama, T. Yoshino, *Bull. Chem. Soc. Jpn.* **1972**, *45*, 481–484.
[17] T. J. Atkins, J. E. Richman, W. Oettle, *Org. Synth.* **1978**, *58*, 86–88.
[18] A. Buttafava, L. Fabbrizzi, A. Perotti, A. Poggi, G. Poli, B. Seghi, *Inorg. Chem.* **1986**, *25*, 1456–1461.
[19] J. E. Richman, T. J. Atkins, *J. Am. Chem. Soc.* **1974**, *96*, 2268.
[20] M. V. Baker, D. H. Brown, B. W. Skelton, A. H. White, *J. Chem. Soc. Dalton Trans.* **2000**, 4607–4616.
[21] L. G. Qian, Z. Sun, J. K. Bowman, *Supramol. Chem.* **1996**, *6*, 313–325.
[22] L. Fabbrizzi, D. M. Proserpio, *J. Chem. Soc. Dalton Trans.* **1989**, 229–232.
[23] M. Kavana, D. R. Powell, J. N. Burstyn, *Inorg. Chim. Acta* **2000**, *297*, 351–361.
[24] D. Reinen, A. Ozarowski, B. Jakob, J. Pebler, H. Stratemeier, K. Wieghardt, I. Tolksdorfi, *Inorg. Chem.* **1987**, *26*, 4010–4017.

[25] P. J. Wilson, A. J. Blake, P. Mountford, M. Schroeder, *Inorg. Chim. Acta* **2003**, *345*, 44–52.

[26] U. Bossek, D. Nuhlen, E. Bill, T. Glaser, C. Krebs, T. Weyhermuller, K. Wieghardt, M. Lengen, A. X. Trautwein, *Inorg. Chem.* **1997**, *36*, 2834–2843.

[27] A. C. Moreland, T. B. Rauchfuss, *Inorg. Chem.* **2000**, *39*, 3029–3036.

[28] G. C. Silver, W. C. Trogler, *J. Am. Chem. Soc.* **1995**, *117*, 3983–3993.

[29] D. Hanke, K. Wieghardt, B. Nuber, R. S. Lu, R. K. McMullan, T. F. Koetzle, R. Bau, *Inorg. Chem.* **1993**, *32*, 4300–4305.

[30] P. L. Luisi, B. E. Straub, *Reverse Micelles. Biological and Technological Relevance of Amphiphilic Structures in Apolar Media*, New York, **1987**.

Received: June 25, 2007